J. Acoust. Soc. Jpn. (*E*) 9, 2 (1988)

Detection of flaws in ball bearings by analysis of vibration signals detected by two pick-ups

Akihiro Yuasa,* Hiroshi Kanai,** Masato Abe,* and Ken'iti Kido*

**Research Center for Applied Information Sciences, Tohoku University, 2-1-1, Katahira, Sendai, 980 Japan*
***Education Center for Information Processing, Tohoku University, Kawauchi, Sendai, 980 Japan*

(*Received 22 May 1987*)

This paper describes a new method for automatic detection of slight flaws on the outer race of a ball bearing using two vibration pick-ups. On production lines of mass-produced precision ball bearings, the detection and classification of flaws on the balls and races have been carried out by aural monitoring of vibration signals of the outer ring. Some useful automatic methods based on the analysis of the periodicity of vibration pulses excited by the flaws have been developed as alternatives to aural inspection. However, slight flaws on the outer race are not always detected by those methods because the vibration pick-up is almost completely insensitive to the vibration due to a flaw in a direction perpendicular to the pick-up point. Therefore, we have developed a new method to detect slight flaws on the outer race, regardless of the position of flaws. With this method, slight flaws are detected from the cross spectrum between the squared envelope signals of the vibration signals detected by two vibration pick-ups.

PACS number: 43. 85. Ta, 43. 60. Gk

1. INTRODUCTION

This paper describes a new diagnostic method for the automatic detection of flaws on the surface of the outer race of a ball bearing. To prevent the generation of harmful vibration, the ball bearings used in precision machines, for example, video tape recorders, should have no flaw larger than a micrometer. Therefore, all the bearings passing through a production line have been inspected by trained workers skilled in the auditory evaluation of vibration signals produced by the outer ring. However, high reliability cannot be expected of such human inspection. Furthermore, a long period, more than three months, is necessary for the training of the inspectors. Therefore, we have developed a new method using two pick-ups for the automatic detection and classification of flaws in ball bearings.[1] If one pick-up is used, flaws are detected at the same accuracy rate as when inspection is done by a skilled worker. However, the resonant vibration due to slight flaws on the outer race cannot be detected by the use of one pick-up when the position of the flaw is at a certain position, because the signal-to-noise ratio is quite low when the vibration pick-up point coincides with the nodal point of the resonant vibration of the outer ring. Therefore, we have developed a new method using two pick-ups.

In this paper, we first describe the apparatus for the experiments. Next, we discuss the reasons why the slight flaws on the outer race cannot be detected by the use of one pick-up or by the conventional cross spectral method. Finally, we propose a new method using the cross spectrum between the envelope signals of the squared magnitude of the narrow band signals detected by two vibration pick-ups. The usefulness of this method is experimentally confirmed.

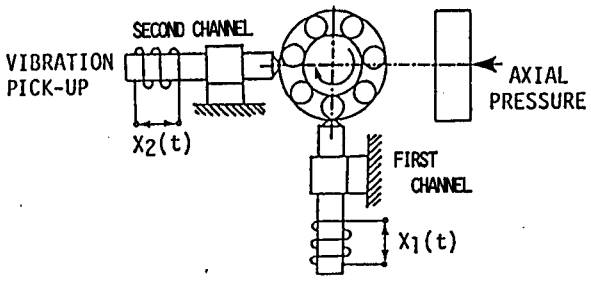

Fig. 1 The procedure for measuring two vibration signals of a ball bearing.

2. APPARATUS FOR THE EXPERIMENTS

Figure 1 shows a block diagram of the procedure for measuring the two channel vibration signals of a ball bearing.[1] The outer ring is fixed by imposing axial pressure, and the inner ring is revolved at a constant speed of 1,800 r.p.m. Under such conditions, a flaw on the race or on the ball causes a radial vibration of the outer ring. Two signals, $x_1(t)$ and $x_2(t)$, are picked up by two vibration pick-ups attached to the outer ring. Each of the signals is A/D converted with a two channel 12 bit A/D converter at a sampling period of 30 μs.

3. MODEL OF THE VIBRATION SIGNALS CAUSED BY A FLAW

A vibration, $x_0(n)$, of the outer ring is excited by a flaw on the outer race, where n is the discrete time. It is assumed in the simplified model that the resonant vibration signal is expressed as the sum of exponentially decaying sinusoidal waves,[1] as follows:

$$x_0(n)=\sum_{i=1}^{M}\exp(-\alpha_i n)\cos(\omega_i n)u(n), \qquad (1)$$

where $u(n)$ is a unit step function, M is the number of the exponentially decaying sinusoidal waves, ω_i is an angular eigen frequency and α_i is a damping factor of i-th mode. Since the inner ring of the bearing is revolved at a constant speed, the vibration signal, $x_0(n)$, repeats at a uniform period, T, the value of the period T depending on the position of the flaw.[2] However, it is known that there is some scattering in the repetition intervals of the flaw pulses generated by many balls since the diameter of the ball is a little smaller than the space in the cage.[1] Therefore, the resultant vibration signal is expressed as follows:

$$\begin{aligned} x(n)&=x_0(n)*r(n)\\ &=x_0(n)*\sum_{k=-N}^{N}\delta(n-kT-\Delta_k), \end{aligned} \qquad (2)$$

where

$$\delta(n)=\begin{cases}1 & (n=0)\\ 0 & (n\neq 0),\end{cases}$$

$r(n)$ is the impulse train, $*$ represents the convolution, and Δ_k represents the lag for the k-th impulse from the expected time, kT. The signals, $x_1(n)$ and $x_2(n)$, picked up by the two sensors shown in Fig. 1 are represented as follows:

$$x_i(n)=C_i\cdot x(n)+n_i(n), \quad (\text{for } i=1,2) \qquad (3)$$

where C_i denotes the real constant determined by the angle between the i-th pick-up and the flaw on the race, and $n_i(n)$ is the observed noise superimposed on the signal detected by the i-th pick-up.

When the point of a vibration pick-up coincides with the nodal point of the resonant vibration of the outer ring, the constant, C_i, has a small value, which causes a poor signal-to-noise ratio. It is necessary to apply a noise compensation technique to detect the resonant vibration caused by the flaw under the condition of such a low signal-to-noise ratio. However, such a flaw cannot be detected by the ordinary cross spectrum method. The cross spectrum, $G(p)$, of the vibration signals, $x_1(n)$ and $x_2(n)$, is represented as follows:

$$\begin{aligned} G(p)&=X_1(p)\cdot X_2^*(p)\\ &=[C_1\cdot X(p)+N_1(p)][C_2\cdot X(p)+N_2(p)]^*\\ &=C_1C_2\cdot|X_0(p)|^2\cdot|R(p)|^2+N_1(p)\cdot N_2^*(p)\\ &\quad+C_1X_0(p)R(p)N_2^*(p)\\ &\quad+C_2X_0^*(p)R^*(p)N_1(p), \end{aligned} \qquad (4)$$

where $X_1(p)$, $X_2(p)$, $X_0(p)$, $R(p)$ and $N_i(p)$ are the spectra of $x_1(n)$, $x_2(n)$, $x_0(n)$, $r(n)$ and $n_i(n)$, respectively, and * denotes the complex conjugate. When there is some scattering in the repetition intervals of the impulse train, $r(n)$, of Eq. (2), it is known that the power spectrum, $|R(p)|^2$, of $r(n)$ in Eq. (4) is composed of line peaks at the frequencies $f=n/T$, $n=1,2,\ldots$, only in the low frequency band.[1] However, in the low frequency range, which is very far from the resonant frequency, the signal-to-noise ratio is very small, and we cannot detect the peaks due to flaws using the conventional cross spectrum method.[1]

Figure 2 shows the results of the cross spectral technique and the cepstral technique. The cross power spectra are calculated by averaging 75 cross

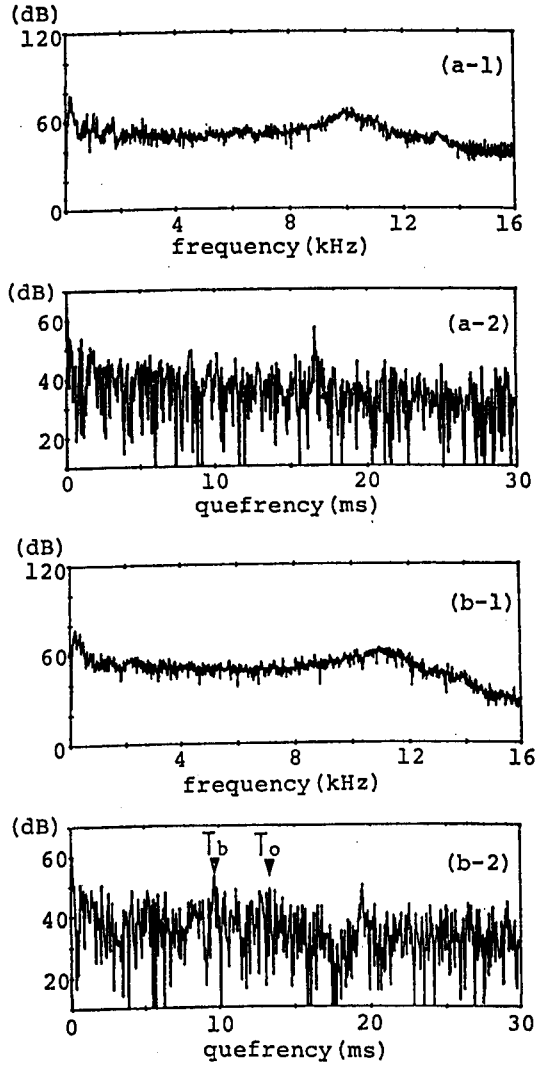

Fig. 2 Results by conventional techniques to detect a flaw. T_o: repetition interval of a flaw pulses driven by the flaw on the outer race. T_b: repetition interval of a flaw pulses driven by the flaw on the ball. (a-1) cross power spectrum (a normal bearing), (a-2) cepstrum (a normal bearing), (b-1) cross power spectrum (a bearing with a flaw on the outer race and on the ball), (b-2) cepstrum (a bearing with a flaw on the outer race and on the ball).

spectra, which are computed after cutting the vibration signal into segments by use of a 2,048-point Hanning window. Figures 2 (a-1) and 2 (a-2) show the results for a normal bearing, and Figs. 2 (b-1) and 2 (b-2) show those for a bearing which has a slight flaw on the ball and a relatively large flaw on the outer race. There is little difference between the cross power spectrum of a normal bearing and a bearing with a flaw on the outer race. Although the bearing shown in Figs. 2 (b-1) and 2 (b-2) has a slight flaw on the ball and a larger on the outer race, we can recognize only a peak at the position corresponding to the periodic interval, T_b, of the flaw on the ball in Fig. 2 (b-2) by the ordinary cepstrum technique. With the cepstrum technique, it is difficult to recognize a peak at the position corresponding to the periodic interval, T_o, of the flaw on the outer race, even if the flaw on the outer race is large.

4. FLAW DETECTION BASED ON THE CROSS SPECTRUM BETWEEN THE ENVELOPE SIGNALS ON THE TWO-CHANNEL NARROW BAND SIGNALS

We propose a new method for detection of vibration signals due to a flaw on the outer race. Each of the two input signals, $x_1(n)$ and $x_2(n)$, is band-limited, using a short-time (16-point) Fourier transform, and eight narrow band-passed signals are obtained. Then, the significant frequency band, by which the optimum detection of flaws is achieved, is selected from the eight narrow bands. An envelope signal is obtained by squaring each of the narrow band-passed signals and by passing them through a low-pass filter. The periodicity of the flaw pulses is detected from the averaged cross spectrum between the two channel envelope signals. The proposed method has two advantages: it removes the effect of the fluctuations of the period, and it emphasizes the resonant vibration components buried in the random noise as explained in the following sections.

4.1 The Reduction of the Influence of the Fluctuation in the Period

By using the narrow band-pass filter where the impulse response is $w(n)$, each of the band-limited signals, $y_i(n)$, $i=1,2$, is expressed as follows:

$$y_i(n)=w(n)*x_i(n)\,. \quad (i=1,2) \tag{5a}$$

The spectrum $Y_i(p)$ of the band-limited signal $y_i(n)$ is represented using Fourier transform $X_i(p)$ of $x_i(n)$ and the transfer function $W(p)$ of a narrow band-pass filter as follows:

$$Y_i(p)=W(p)\cdot X_i(p)\,. \tag{5b}$$

Using the relation $F[y^*(n)]=Y^*(-p)$, where $F[\ ]$ denotes the Fourier transform and $y^*(n)$ and $Y^*(-p)$ denote the complex conjugates of $y(n)$ and $Y(-p)$,

respectively, the spectrum $Z_i(p)$ of the squared band-passed signal $z_i(n)=|y_i(n)|^2$ is represented as follows:

$$\begin{aligned}Z_i(p)&=F[y_i(n)y_i^*(n)]\\&=F[y_i(n)]*F[y_i^*(n)]\\&=Y_i(p)*Y_i^*(-p)\\&=\sum_{k=-N}^{N-1}Y_i(k)Y_i^*(k-p)\\&=\sum_{k=-N}^{N-1}W(k)X_i(k)W^*(k-p)X_i^*(k-p),\end{aligned}\tag{6}$$

since $z_i(n)$ is the squared signal, the spectrum $Z_i(p)$ has low frequency components. From Eq. (3), the spectrum $X_i(p)$ is the sum of two components: the resonant vibration $X_i(p)=C_iX(p)$ and a random noise $N_i(p)$, as follows:

$$X_i(p)=C_iX(p)+N_i(p).\tag{3'}$$

Using Eqs. (6) and (3'), $Z_i(p)$ is represented as follows:

$$\begin{aligned}Z_i(p)=&\sum_{k=-N}^{N-1}W(k)W^*(k-p)\\&\times\{C_i^2X(k)X^*(k-p)+C_iX(k)N_i^*(k-p)\\&+C_iN_i(k)X^*(k-p)+N_i(k)N_i^*(k-p)\}.\end{aligned}\tag{7}$$

In Eq. (7) the components due to the second term $C_iX(k)N_i^*(k-p)$ and the third term $C_iN_i(k)X^*(k-p)$ take small values since there is no correlation between $X(k)$ and $N_i(k)$. From other experiments, we found the fact that the resonant signal $x(n)$ due to flaws has a broad-phase characteristic in the frequency domain, while the noise $n_i(n)$ has a random-phase characteristic. Thus, $Z_i(p)$ is represented as follows:

$$\begin{aligned}Z_i(p)=&\sum_{k=-N}^{N-1}W(k)W^*(k-p)\\&\times\{C_i^2X(k)X^*(k-p)+N_i(k)N_i^*(k-p)\}\\=&F[|w(n)*C_ix(n)|^2]\\&+F[|w(n)*n_i(n)|^2].\end{aligned}\tag{8}$$

Thus, the squared signal, z_i, has low frequency components due to the resonant vibration when the frequency components around the central frequency of the resonant vibration are in the passed band of the filter $w(n)$.

Other investigations[1] have shown the length of response, $x_0(n)$, of Eq. (2) to a flaw and the duration $2N$ of $w(n)$ to be sufficiently shorter than the period of the repetition interval T. Thus, the term $|w(n)*C_ix(n)|^2=C_i^2|w(n)*(x_0(n)*r(n))|^2$ is approximated by $C_i^2|w(n)*x_0(n)|^2*|r(n)|^2$. Therefore, $Z_i(p)$ is represented as follows:

$$\begin{aligned}Z_i(p)=&C_i^2F[|w(n)*x_0(n)|^2*|r(n)|^2]\\&+F[|w(n)*n_i(n)|^2]\\=&C_i^2X_0'(p)\cdot R(p)+N_i'(p),\end{aligned}\tag{9}$$

where $X_0'(p)$, $R(p)$ and $N_i'(p)$ are the spectra of $|w(n)*x_0(n)|^2$, $|r(n)|^2$ and $|w(n)*n_i(n)|^2$, respectively.

Therefore, the cross spectrum, $G_e(p)$, of the two squared signals, $z_1(n)$ and $z_2(n)$, is expressed as follows:

$$\begin{aligned}G_e(p)=&Z_1(p)Z_2^*(p)\\=&(C_1C_2)^2|X_0'(p)|^2\cdot|R(p)|^2+N_1'(p)N_2'^*(p)\\&+C_1^2X_0'(p)R(p)N_2'^*(p)\\&+C_2^2X_0'^*(p)R^*(p)N_1'(p).\end{aligned}\tag{10}$$

Thus, even if the original resonant vibration, $x_0(n)$, does not contain low frequency components, the low frequency components of $|X_0'(p)|^2$ are large in magnitude, and $G_e(p)$ shows clear peaks at low frequencies.

4.2 The Emphasis of the Resonant Vibration Components

For the cross spectra of the squared envelope, signals are calculated for M segments and are averaged. Since the power of the first term of Eq. (10) has a positive value and has the same characteristics for every section, the averaged cross spectrum is described as follows:

$$\begin{aligned}G_e(p)=&\frac{1}{M}\sum_{m=1}^{M}G_e(p:m)\\=&(C_1C_2)^2|X_0'(p)|^2\cdot|R(p)|^2\\&+\frac{1}{M}\sum_{m=1}^{M}[N_1'(p:m)N_2'^*(p:m)]\\&+\frac{1}{M}C_1^2X_0'(p)R(p)\sum_{m=1}^{M}N_2'^*(p:m)\\&+\frac{1}{M}C_2^2X_0'^*(p)R^*(p)\sum_{m=1}^{M}N_1'(p:m),\end{aligned}\tag{11}$$

where $G_e(p:m)$ is the cross spectrum for the m-th segment, and $N_i'(p:m)$ denotes the spectrum of $|n_i(n)*w(n)|^2$ for the m-th segment. In Eq. (11), the components due to the second, the third and the fourth terms have small values at $p\neq0$ since $N_i'(p:m)$ has random values for different m's, and there is

no correlation between $N_1'(p:m)$ as shown in the experiments described below.

Figure 3 (a-1) shows the coherence of the vibration signals from a normal bearing, and Fig. 3 (b-1) shows that of the vibration signals excited by a flaw on the outer race. Since the resonant vibration is excited by flaws, the vibration signals for the normal bearing have only noise components. Therefore, the cross spectrum, $G_e(p)$, of the normal bearing may be equal to the second term of Eq. (11).

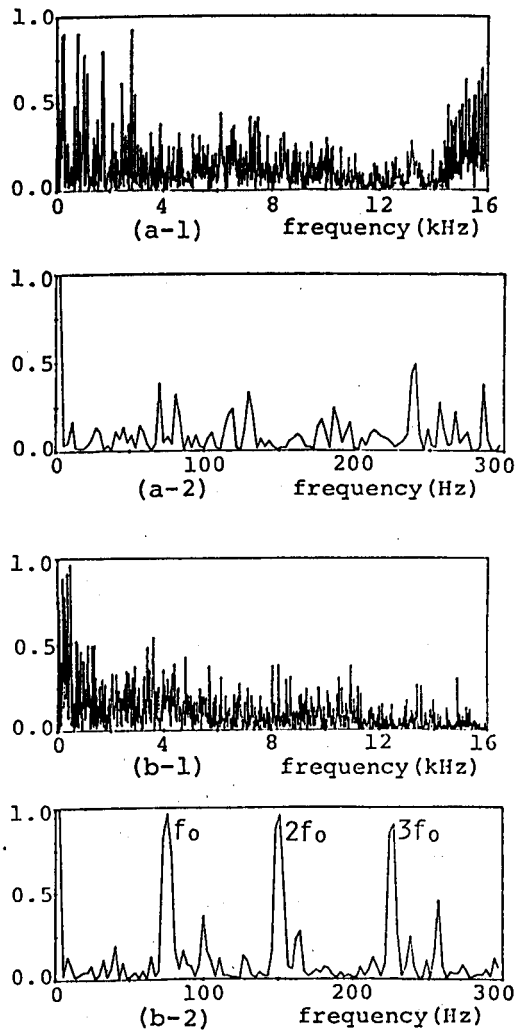

Fig. 3 The coherences between the vibration signals picked up by the first and the second channels. (a-1) coherence between the vibration signals (a normal bearing), (a-2) coherence between the envelope signals of the squared magnitude of the original vibration signals (a normal bearing), (b-1) coherence between the vibration signals (a bearing with a flaw on the outer race and on the ball), (b-2) coherence between the envelope signals of the squared magnitude of the original vibration signals (a bearing with a flaw on the outer race and on the ball).

Figures 3 (a-2) and 3 (b-2) show the coherence functions between the squared signals for a normal bearing and a bearing with a flaw on the outer race, respectively. Figure 3 (a-2) shows that the coherence function has small values at all frequencies, and Fig. 3 (b-2) shows that the coherence function also has small values except for the frequencies $f=n/T$, $n=0,1,2,\ldots$, which are the frequencies due to the periodic interval of the flaw. This means that there is little correlation between noise $N_1'(p:m)$ and $N_2'(p:m)$. Furthermore, $N_i'(p:m)$ has a different value for different m's. Therefore, an averaged cross spectrum is described as follows:

$$G_e(p)=(C_1C_2)^2|X_0'(p)|^2|R(p)|^2. \quad (p\neq 0, M\to\infty) \tag{12}$$

Equation (12) means that the signal to noise ratio can be increased by using the cross spectrum technique for squared signals.

Next, we discuss the noise reduction rate by use of the cross spectral technique using the squared envelope signals: Letting the variances, $N_1'(p:m)\cdot N_2'^*(p:m)$ and $X_0'(p)N_i'(p:m)$, have constant values, σ_{NN}^2 and σ_{SN}^2, the resultant variances by averaging M times become σ_{NN}^2/M and σ_{SN}^2/M, respectively.

$G_e(p)$ has the dimension of the squared power. Therefore, the signal to noise ratio is improved by 2.5

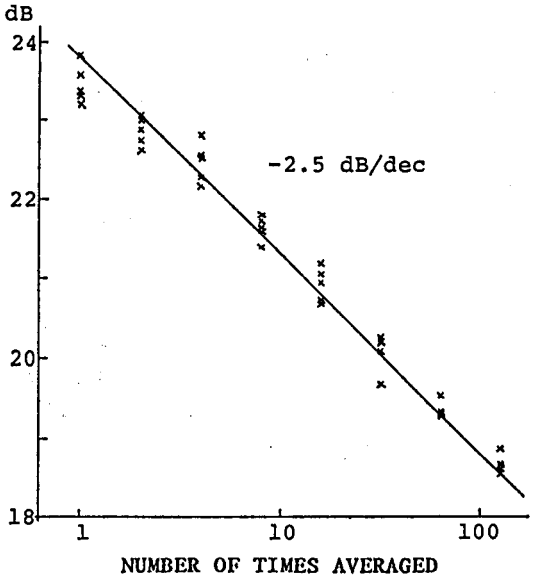

Fig. 4 Reduction of the noise in the cross spectrum between squared envelope signals by averaging.

dB with ten-fold averaging. Figure 4 shows the relation between the degree of averaging and the noise reduction rate obtained by computer simulation. The result shown in this figure is the same as that based on theoretical considerations.

5. EXPERIMENTS AND RESULTS

The following is the process of the flaw detection method utilizing the proposed method as outlined in this paper: First, each of the two signals is divided into many segments by multiplying the signal by the short time (16-point) Hanning window. Adjacent segments overlap by a half-length. Each of them is band-limited by calculating the Fourier transform. Each of the band-limited signals is squared and moving-averaged using a 16-point Hanning window so that only low frequency components due to flaws are extracted. Then, two squared envelope signals are obtained by selecting a sample from every third segment, and the period of the flaws is estimated from the two envelope signals by the cross spectrum technique using the FFT (512-point Hanning window, average of the sum of 23 cross spectra).

Figure 5 shows the experimental results obtained by the proposed method. Figures 5 (a) and 5 (b) show the averaged power spectra and the averaged cross spectra, $G_e(p)$, of the squared envelope signals for a bearing with a slight flaw on the outer race. The vibration signals used in Fig. 5 (a) are the same as those used in Fig. 2. The quantity θ [degree] denotes the angle between the first pick-up and the flaw. In Fig. 5 (a), peaks are seen to appear clearly at the frequencies f_o, $2f_o$ and $3f_o$, which coincide with the theoretical frequencies. On the other hand, these peaks cannot be observed by the conventional cross spectrum technique and the cepstrum technique as shown in Fig. 2. When the flaw is far from the pick-up ($\theta = 112.5$ degree), clear peaks are not observed from the power spectrum of the squared envelope signal of the vibration signal as shown in Fig. 5 (b-1) or 5 (b-2). However, clear peaks can be obtained in the cross spectrum at the frequencies f_o, $2f_o$ and $3f_o$ as shown in Fig. 5 (b-3). Figure 6 shows the results obtained from the signals of a normal bearing. Clear peaks are not observed in the three spectra. Therefore, the existence of flaws is determined by checking whether or not there are peaks at the frequencies f_o, $2f_o$ and $3f_o$.

Next, the effect of the relation between the position of the pick-ups and the flaw on the outer race is investigated. That is, the positions of the pick-ups are fixed and that of the flaw on the outer race is changed, and the power, $P(f_o:\theta)$, of the peak appearing at f_o in the cross spectrum, $G_e(p)$, and the

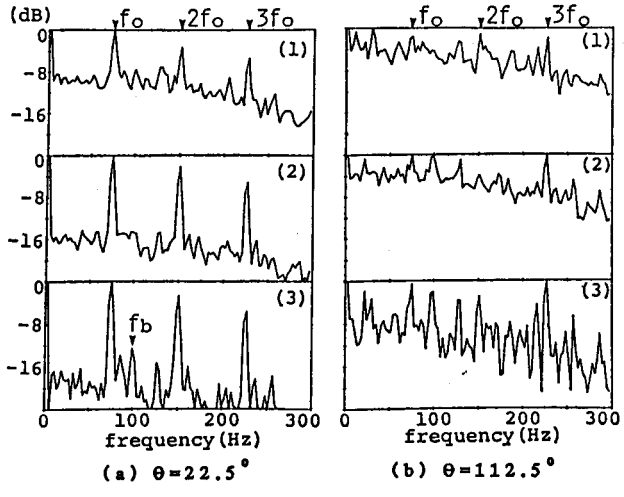

Fig. 5 The power spectra and the cross power spectrum between the squared envelope signals of the vibrations caused by a slight flaw on the outer race (θ is the angle between the flaw and the first pick-up). (1) power spectrum (first channel), (2) power spectrum (second channel), (3) cross spectrum, $G_e(p)$.

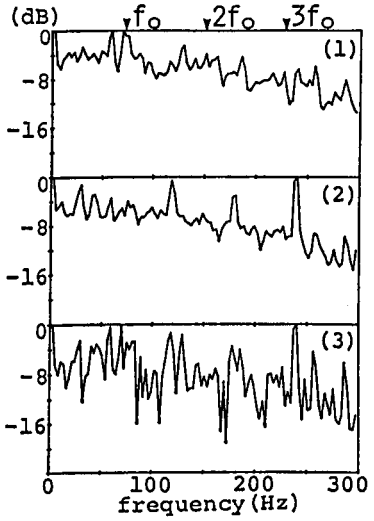

Fig. 6 The averaged power spectra and averaged cross spectrum between the squared envelope signals of the vibrations detected from a normal ball bearing. (1) power spectrum (first channel), (2) power spectrum (second channel), (3) cross power spectrum, $G_e(p)$.

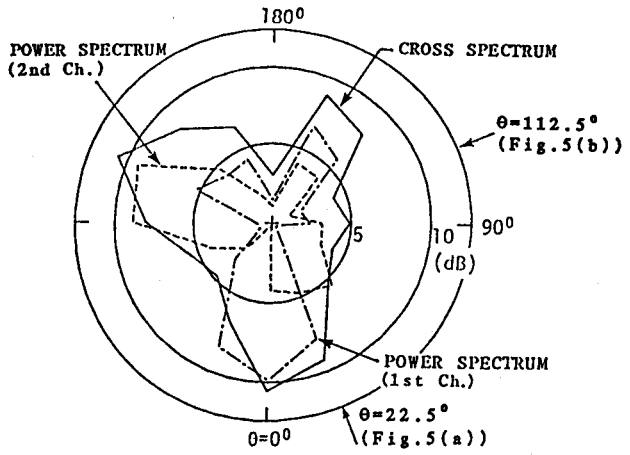

Fig. 7 The power, $P(f_0:\theta)$, of the peak appearing at the repetition frequency f_0 in the power spectra and the cross power spectrum between the squared envelope of the vibrations signals.

power spectra of the squared envelope signals are calculated. Figure 7 shows the result. Clear peaks due to the flaw at $\theta=90°$ can be observed only by the cross spectrum, where the flaw is far from each pick-up. In such a case, the flaw cannot be detected by a skilled inspector nor by the conventional method.

6. CONCLUSIONS

A new method, in which the vibration signals are detected with two vibration pick-ups, is proposed for the automatic detection of slight flaws in ball bearings. This method has been developed to detect a slight flaw on the outer race, even if the flaw is in a direction perpendicular to the direction of the pick-up. It is confirmed by experiments that slight flaws on the outer race, which are not detected by other methods including inspection by a skilled worker, are detected by our new method.

REFERENCES

1) H. Kanai, M. Abe, and K. Kido, "Detection and discrimination of flaws in ball bearings by vibration analysis," J. Acoust. Soc. Jpn. (E) **7**, 121–131 (1986).
2) S. Braun and B. Datner, "Analysis of roller/ball bearing vibrations," Trans. Am. Soc. Mech. Eng., J. Mech. Des. **101**, 118–125 (1979)